CHAPTER 4

RESULTS AND DISCUSSION

4.1   Temperature inside crucible

Temperature inside crucible was measured in comparison with that of outside crucible, which was equal to the furnace temperature, at the conditions of heating rate 10 ^{o}C/min and holding temperature at 1600 ^{o}C. The measured values are shown in appendix Table B-1. Fig 4.1 shows the temperatures as a function of time (min). Temperature inside furnace was almost the same with that of programmed temperature.
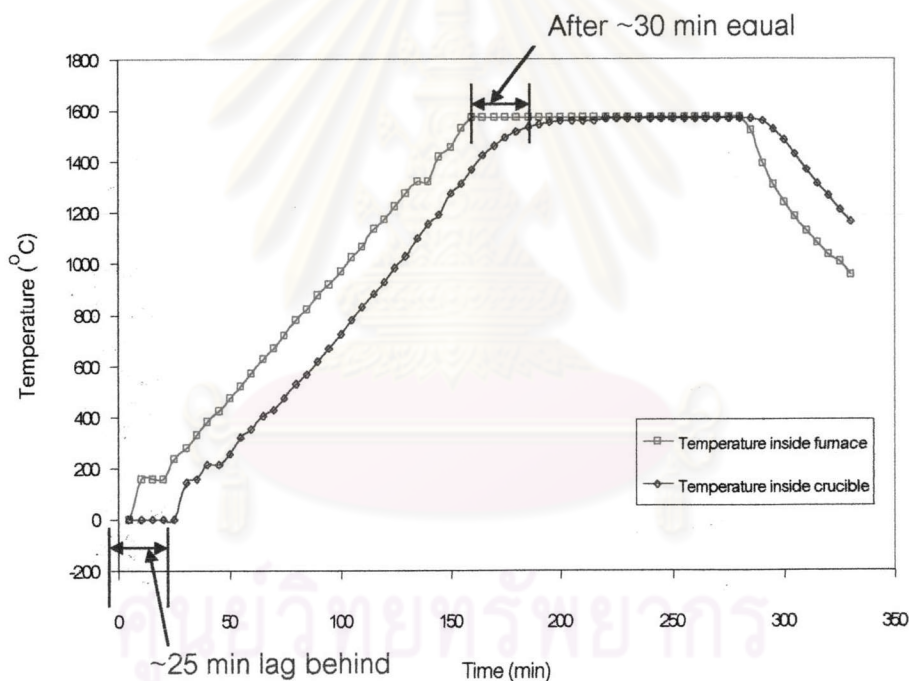

Fig 4.1 Relationship between the temperature inside the furnace and inside the crucible versus time

As shown in Fig 4.1, the delay of temperature inside Al_2O_3 crucible was observed. The temperatures inside crucible increased with slower rate than outside

crucible about 25 min. However, both inside and outside temperatures of crucible became the same after about 30 min, soaking.

4.2   Particle size distribution of powders

Two kinds of Si_3N_4 mixed powders and four kinds of Si_3N_4 packing powders, which are powder A, powder B, SN-E10, SN-7, SN-KO5, and SN-F2 were investigated in this study. Particle size distribution curves are shown in Appendix B-1. Particle size distribution data and curve measured by sieve analysis are shown in Appendices B-2 and B-3. Table 4.1 shows average particle size of Si_3N_4 powders.

As in the appendix, particle size distribution curves of Al_2O_3 packing powders, which are AM-21 and A-11, are also plotted in Fig B-2. Average diameters of A-11 and AM-21 powder are 2.87 μm and 9.02 μm, respectively. In case of A-11, the size of powder that measured by sedimentation analysis is smaller than the specification. It is supposed that the size of powder from supplier was not measured directly but agglomerate particle size was reported.

Table 4.1 Average particle size of powders

Type of sample	Average particle size (μm)
Mix powder A	0.69
Mix powder B	0.61
SN-E10	0.83
SN-7	3.40
SN-KO5	1.68
SN-F2	21.71
AM-21	2.87
A-11	9.02

4.3   Outlook observation of specimen and packing powder

4.3.1   Mixed powder A

The features of packing powder, which are SN-E10, SN-7, SN-7 mixed with BN and Al_2O_3, after sintering at temperatures in the range from 1550 to 1700 ^{0}C are shown in appendix Table B-3.

Comparing C1 and C2 condition, it is understood that the agglomeration of Si_3N_4 packing powder strongly depends on the kind of powder. SN-7 strongly agglomerated and made a lid stick to small Al_2O_3 crucible (C1). SN-E10 did not show serious agglomeration (C2). Al_2O_3 packing powder, AM-21 in both C1 and C2 conditions agglomerated and stuck strongly to the small Al_2O_3 crucible. Then, AM-21 and SN-7 powder were replaced by A-11 and SN-7 mixed with 10 mass % of boron nitride (BN) in the following conditions (C3 to C13) to decrease agglomeration behavior.

Comparing the agglomeration of SN-7 and SN-7 mixed with BN powder, agglomeration and lid stick of SN-7 mixed with BN were less than that of SN-7. SN-7 mixed with BN powder. However, BN powder easily oxidized and formed B_2O_3 as a glassy phase.[42] As a result, SN-7 mixed with BN powder gave strong surface layer as shown in Fig 4.2. On the contrary, in case of SN-E10 (C4, C6, C8, C10, C12 and C13 conditions) weak agglomerations were observed. This phenomenon was probably related to raw material properties in Appendix Table A-1 and Table 3.3. Weak agglomeration of SN-E10 related to low tap density. In case of Al_2O_3 packing powder, A-11 still agglomerated but less than AM-21. As seen in Table 3.4, A-11 is coarser than AM-21 and tap density of A-11 is smaller than that of AM-21. Therefore, A-11 is a better material for using as a packing powder.

Fig 4.2a, 4.2b and 4.2c show surface layer (scale) of Si_3N_4 packing powder. Difference in thickness of top part when using different heating rate was observed. When slow heating rate (5^0/min) was performed, the thickness of oxide scale increased. Thin oxide scale was observed when rapid heating rate (10^0/min) was used. This oxide scale at the top surface of small crucible implies that B_2O_3 in the Si_3N_4 packing powder

reacted with oxygen in atmosphere and formed B_2O_3 liquid layer as a glassy phase. Theis glassy phase still remained when cooling. However, peak of B_2O_3 was not detected by X-ray diffraction because of the amorphous nature.

Moreover, thick oxide scale occurred at low temperature than at high temperature. As mentioned in 2.4, reaction (2) occurs during sintering. Fig 1 in Appendix C shows the relation between SiO (g) pressure and temperature. P_{SiO} (g) became higher at high temperature. Therefore, The SiO (g) diffused out from inside the small crucible and disturbed the oxidation of BN and Si_3N_4 at high temperature. Therefore thin oxide scale was observed at high temperature. In addition, phase analysis by X-ray diffractometer was performed to confirm the reaction during sintering. Table E-4.5 show that bottoms part of Si_3N_4 packing powders consisted of α and β only, on the contrary, cristobalite was observed at the top part as minor phase. These results confirmed that SiO_2 generated from Si_3N_4 to the top part of packing powders.

4.3.2 Mixed powder B

Table B-4 in appendices and Fig 4.2 show the result of SN-KO5, SN-F2 and A-11 packing powders after sintering at temperatures 1650 to 1700 $^{\circ}$C for 1 and 2 h.

Under E1 and E2 conditions, which are sintered at 1650 $^{\circ}$C for 2 h, thick oxide scale with crack on the top and weak agglomeration of bottom part were observed. This was opposite to SN-F2 powders, which exhibited thin layer of oxide scale, consisted with glass bubble and strong agglomeration at the top surface. Base on the data in Table A-2, high agglomeration of SN-F2 came from wide range of particle size diameters, which was easily to get high packing density. Another reason was related to tap density and specific surface area as shown in Table 3.3. Since SN-F2 had high specific surface area and high tap density, high agglomeration occurred.

Under conditions of E3 to E10, which were sintered at 1700 $^{\circ}$C for 1 and 2 h, most of SN-KO5, and SN-F2 demonstrated similar result as E1 and E2 conditions. However, thick oxide layer was observed when soaking time was increased from 1 to

2 h. as shown in Fig 4.2c and 4.2e, respectively. In this case, sintering time was affected with oxidation reaction between Si_3N_4 and oxygen as that of powders A experiment. Taking long sintering time, much amount of oxygen could react with Si_3N_4 and create thick oxide scale.
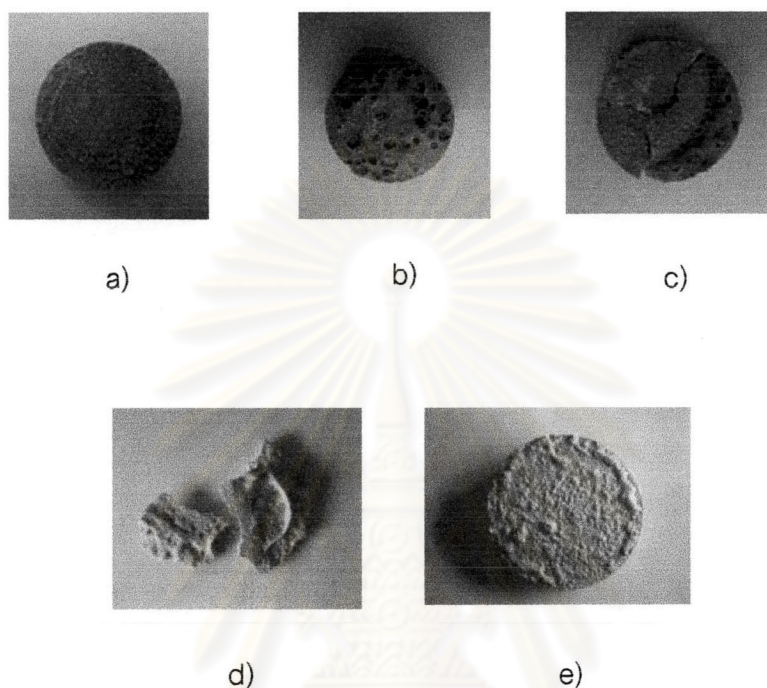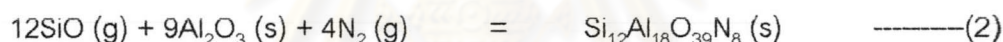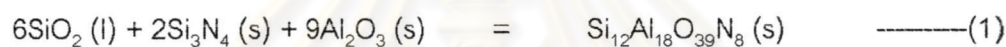

Fig 4.2 Aspects of packing powder after sintering at various conditions. a) SN-7+BN sintered at 1550 ^{o}C, 2 h, 5 ^{o}C/min. b) SN-7+BN sintered at 1600 ^{o}C, 2 h, 5 ^{o}C/min. c) SN-7+BN sintered at 1600 ^{o}C, 2 h, 10 ^{o}C/min. d) SN-F2 sintered at 1700 ^{o}C, 1 h, 10 ^{o}C/min. e) SN-F2 sintered at 1700 ^{o}C, 2 h, 10 ^{o}C/min.

4.4 Deterioration of Al_2O_3 crucible

The whole inside wall of Al_2O_3 crucible changed color to gray after several times of sintering. Furthermore, small amount of powder stuck to the wall of Al_2O_3 crucible with weak bonds and made thin layer. Phase analysis by X-ray diffraction exhibited three types of materials, Si_3N_4, corundum, and Aluminum Silicon Oxide Nitride ($Si_{12}Al_{18}O_{39}N_8$) as shown in Appendix E.

The sample powder was gathered by scratching the inner surface of crucible. Therefore, Si_3N_4 came from packing powder and corundum from Al_2O_3 crucible. Aluminum Silicon Oxide Nitride was supposed to come from either of the following reactions.

$$6SiO_2 \text{ (l)} + 2Si_3N_4 \text{ (s)} + 9Al_2O_3 \text{ (s)} = Si_{12}Al_{18}O_{39}N_8 \text{ (s)} \quad \text{--------(1)}$$

$$12SiO \text{ (g)} + 9Al_2O_3 \text{ (s)} + 4N_2 \text{ (g)} = Si_{12}Al_{18}O_{39}N_8 \text{ (s)} \quad \text{--------(2)}$$

On the surface of Al_2O_3 crucible, there was not so much SiO_2 (l). And it must be difficult thinking the reaction between solid (Si_3N_4) to solid (Al_2O_3). On the contrary, SiO and N_2 are both gases. Then, reaction (2) might be more possible. Al_2O_3 crucible cracked after using several times. The difference of thermal expansion between $Si_{12}Al_{18}O_{39}N_8$ (s) and Al_2O_3 may cause those cracks.

4.5 Mass change

4.5.1 Mixed powder A

Original detail was shown in Appendix Table D-1. The relationship between mass change and temperature is shown in Fig 4.3.
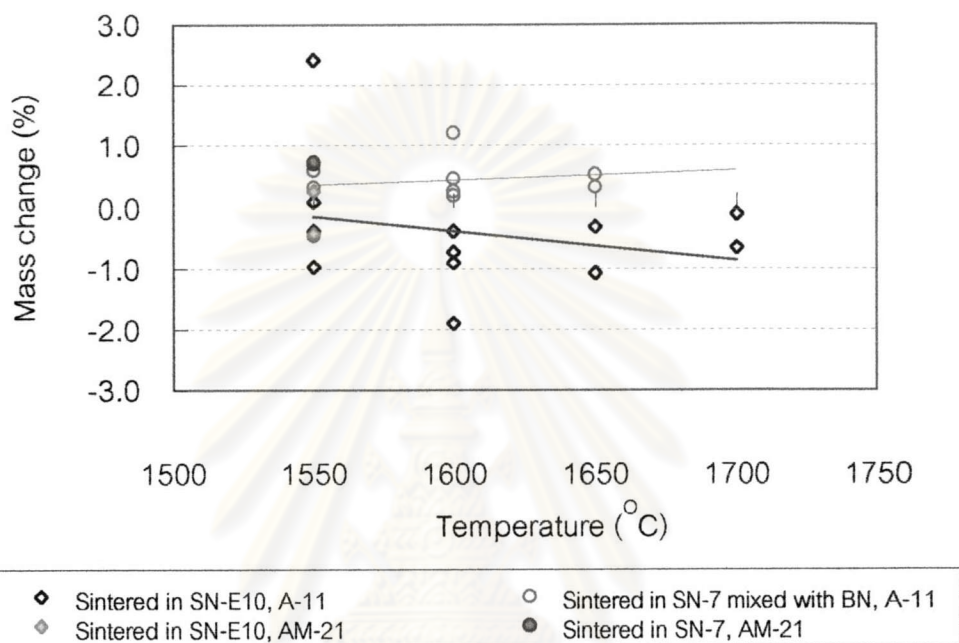

Fig 4.3 Mass change of mixed powder A specimens sintered in each packing powder as a function of temperature

The tendency was that there was mass gain at low temperature as 1550 $^{\circ}$C and 1600 $^{\circ}$C, on the contrary there was a mass loss at high temperature as 1650 $^{\circ}$C and 1700 $^{\circ}$C. Mass gain will be resulted from the following equation.[43]

$$Si_3N_4 \text{ (s)} + 3\, O_2 \text{ (g)} \rightarrow 3\, SiO_2 \text{ (l)} + 2N_2 \text{ (g)} \quad \text{-------- (A)}$$

On the contrary, mass loss (minus value) is presumed to be the following reaction:[18-22]

$$Si_3N_4 \text{ (s)} + 3\, SiO_2 \text{ (l)} \rightarrow 6\, SiO \text{ (g)} + 2\, N_2 \text{ (g)} \quad \text{-------- (B)}$$

4.5.2   Mixed powder B

Fig 4.4 shows mass change of mixed powder B. Original data is in Appendix Table D-2. Both sintered specimens in SN-KO5 and SN-F2 as packing powders exhibited mass loss. The mass loss values are same as those of powder A experiment in E-10 packing powder.
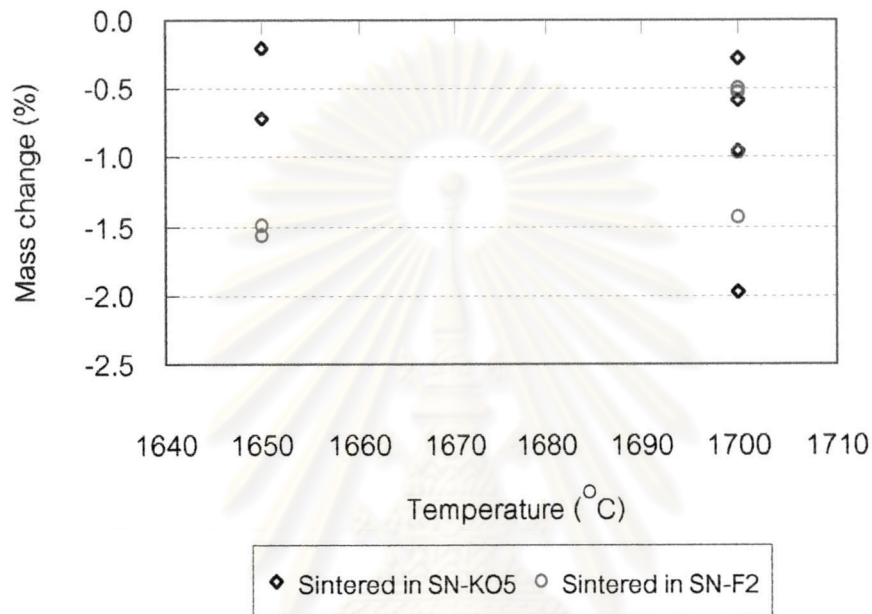

Fig 4.4 Mass change of mixed powder B specimens sintered in each packing powder as a function of temperature

In the early stage of sintering, there are some amounts of oxygen. Then Si_3N_4 is oxidized by the reaction A, and when reaction A occurs, mass gain.

The SiO (g) pressure depends on temperature. The relationship between SiO (g) and temperature is shown in Appendix C, Fig 1. When sintering temperature is high, SiO (g) pressure becomes high. So the reaction B progresses to right side. The SiO_2 is consumed and mass losses. On the contrary, when temperature is low, SiO (g) pressure is low. Then reaction B does not progress so much. Therefore, once the mass gained occurs, it dose not decrease.

At high temperatures (1650 ^{o}C and 1700 ^{o}C), the mass change was positive for SN-7 mixed with BN packing powder, on the other hand it was negative for SN-E10. As seen in Fig 4.2, a hard agglomeration generated on the surface of SN–7 mixed with BN packing powder. On the other hand, almost no such surface layer was observed for SN-E10. When SN-7 mixed with BN was used as packing powder, the SiO (g) of the reaction B could not flow out from the crucible because it was stopped by the surface layer. Then, reaction B did not progress so much. As a result, mass loss was not observed for SN-7 mixed with BN packing powder.

4.5.3   Influence of particle size diameters of SN-F2 packing powder

Powder size distribution of SN-F2 is shown in Appendix Fig B-3. The powder was sieved. Coarse powder (> 75 μm) and fine powder (< 45 μm) were used as packing powder. Mass loss for each powder is shown in Table 4.2.

Table 4.2 Mass change of SN-F2 packing powder after sintering at 1650 ^{o}C

Packing Powder	Sample No.	Mass change (%)	
		Coarse	Fine
SN-F2	1	-0.78	-0.96
	2	-0.67	-0.94

Mass loss of specimen sintered using fine powder was a little higher than that of coarse powder. The reason has not yet been clarified. But the difference is small. Therefore, we think that the difference of particle size of packing powder does not affect the mass loss seriously.

4.6. Bulk density and relative density

4.6.1 Mixed powder A

Fig 4.5 shows the relation between the temperature and bulk density. The bulk densities of specimens sintered and packed with SN-E10 powder were higher than those with SN-7 at over 1600 $^{\circ}$C. This relation is the same as mass loss, which is shown in Table D-1. That is, specimens with much amount of mass loss (SN-E10) are higher in bulk density compared to the others (SN-7 mixed with BN) at the same sintering temperature.
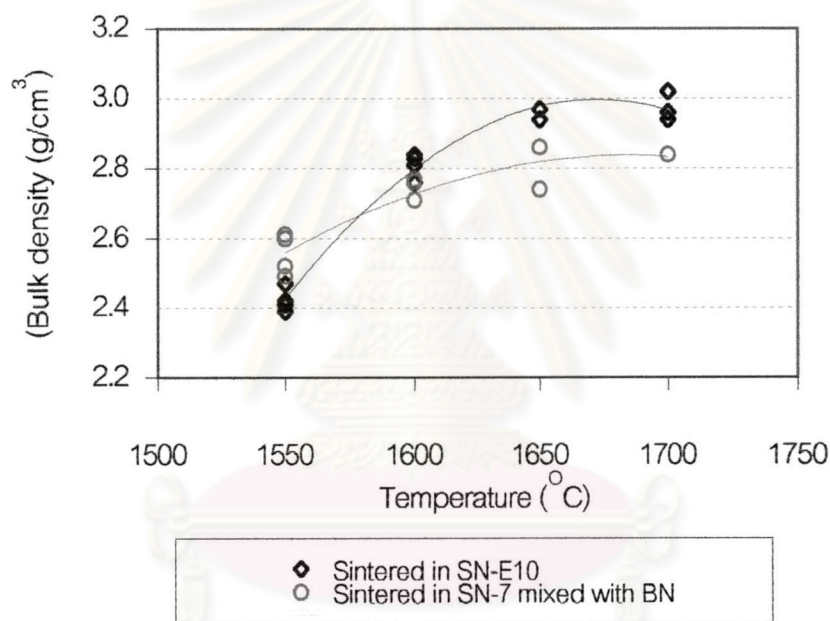

Fig 4.5 Bulk density of mixed powder A specimens

One of the causes of this is thought as follows. When the amount of SiO_2 in the specimen is high, mass loss is high. The true density of specimen depends on the composition as calculated in 3.3.2d). The true density of mixed powder A and B were estimated in Table 3.7. As seen in Table 3.7 the density decreases when SiO_2 content increases. Therefore, the specimen packed with SN-E10 powder showed higher density because much amount of SiO_2 evaporated.

4.6.2   Mixed powder B

Bulk densities of specimens sintered at 1650-1700 ^{o}C with SN-KO5 and SN-F2 packing powder are shown in Fig 4.6. According to bulk density data in Appendix Table D-2, powder B specimens reached to almost full density.
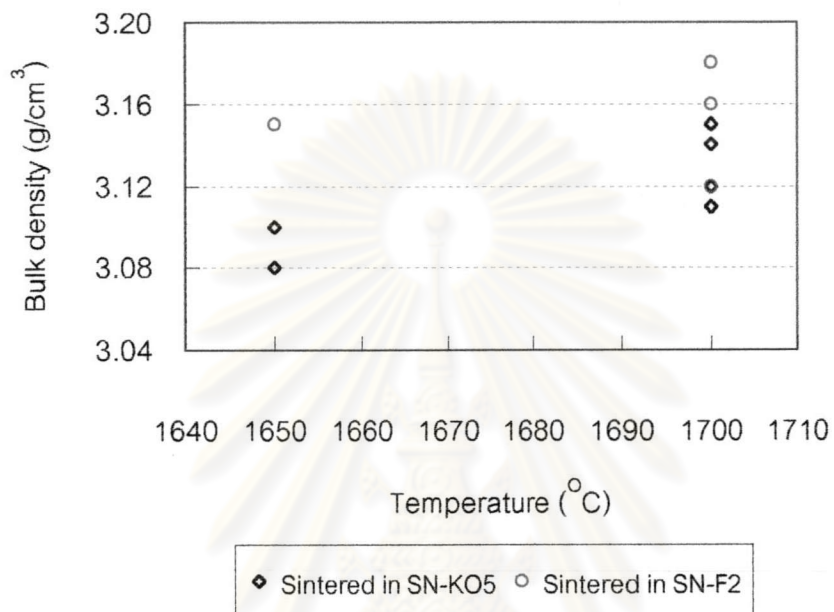

Fig 4.6 Relative density of mixed powder A specimens

Comparing the bulk density of specimens sintered at 1650 ^{o}C for 2 h with SN-F2 and SN-KO5 packing powder, specimens in SN-F2 showed higher density. The cause is same as discussed in 4.6.1.

4.6.3   Influence of particle size diameters of SN-F2 packing powder.

Bulk density and relative density of mix powder B specimens, which were sintered in coarse and fine SN-F2 packing powder, are shown in Table 4.3.

Table 4.3 Bulk densities and Relative densities of mixed powder B, with fine and coarse particle of SN-F2 packing powder at 1650 $^{\circ}$C

Packing Powder	Sample No.	Bulk density (%)		Relative density (%)	
		Coarse	Fine	Coarse	Fine
SN-F2	1	3.16	3.19	96.8	97.8
	2	3.18	3.19	97.4	97.7

The bulk densities and relative densities of specimens, which were sintered in coarse powder, were lower than those in fine powder. Comparing the results with the amount of mass loss shown in Table 4.2, specimens with higher mass loss show higher density. This is the same tendency with the relation between Fig 4.3, Fig 4.4, Fig 4.5, and Fig 4.6.

4.7   Phase content in raw materials, packing powders and specimens

4.7.1   Raw material

α-Phase content of raw material is shown in Table 4.4. α-Phase of SN-E10, SN-7, SN-7mixed with10 mass % BN, and SN-KO5 are 100, 79, 73 and 82 (mass %), respectively. On the contrary, α-Phase content of SN-F2 is only 3 mass %. That is, the powder is almost β-Si_3N_4. Since SN-E10 is the raw powder of mixed powder A and B, α-Phase content of mixed powders are almost 100 % α-Si_3N_4.

Table 4.4 α-Phase content of raw material

Materials	α-phase (mass %)
SN-E10	100
SN-7	79
SN-7 mixed with 10 Wt % of BN	73
SN-KO5	82
SN-F2	3
Mixed powder A	100
Mixed powder B	99

4.7.2   Packing powder

4.7.2.1 Mixed powder A

As shown in Fig 4.2, a hard and agglomerated surface layer generated in packing powder. Then, top and bottom parts of packing powder were analyzed separately. Appendix Table E-1 presents the α / β ratio of each separate part of packing powder. In case of SN-7 mixed with 10 mass % BN sintered at 1650 ^{o}C to 1700 ^{o}C, α-phase (mass %) showed big change from 61 to 88. On the contrary, α-phase of SN-E10 packing powder showed almost no change. Fig 4.7 shows the relationship between α-phase (mass %) and sintering temperature. This result indicated that α transforms to β not so much.
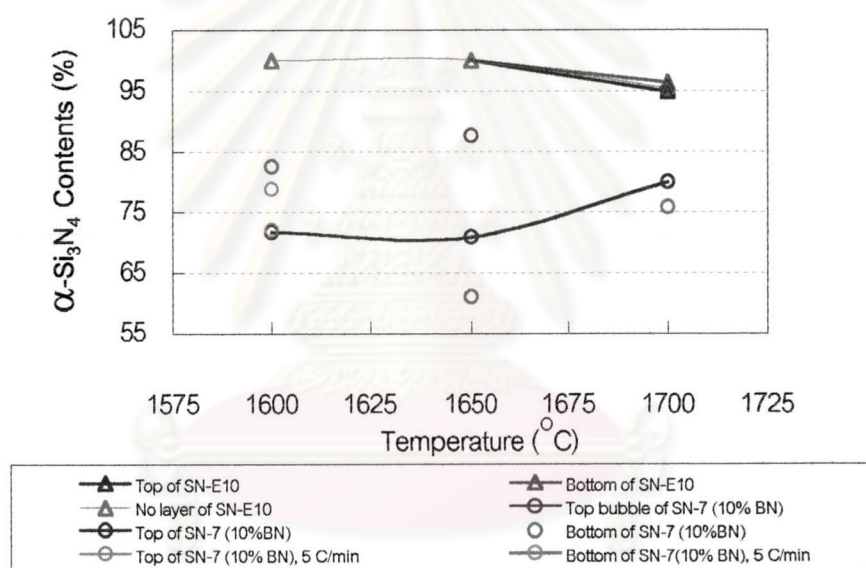
Fig 4.7 Alpha content of SN-E10 and SN-7 mixed with 10 mass % BN packing powders

Appendix, Table E-3 shows α, β-Si_3N_4 and the third minor phases. The phase (X_1-phase) was observed in the condition heated at slow heating rate (5 ^{o}C / min) of SN-E10 and in the top part at elevated temperature (1700 ^{o}C). In case of SN-7 mixed with BN powder similar results was shown, X_1-phase was observed only in top part at low temperature (1600 ^{o}C). For these facts, it was thought that X_1 phase might be easy to generate at low temperature and almost of them change to glassy phase (amorphous) at elevated temperature. X_1-phase was identified as cristobalite phase (SiO_2).

4.7.2.2 Mixed powder B

α / β ratio of SN-KO5, and SN-F2 packing powders are shown in Appendix Table E-2. Fig 4.8 shows the relationship between α-phase (mass %) and temperature of both SN-KO5 and SN-F2 packing powders.
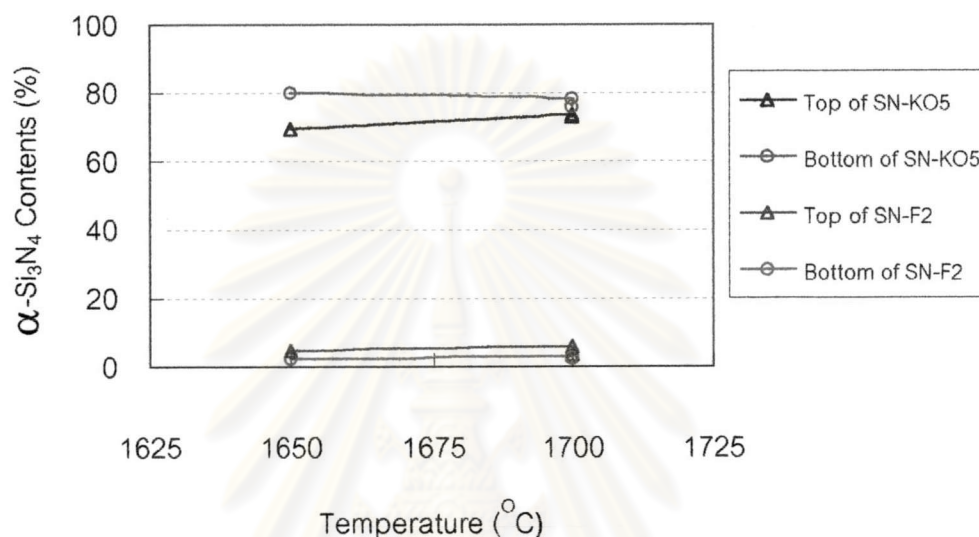

Fig 4.8 Alpha content of SN-KO5 and SN-F2 packing powders

As seen in Table E-2, top layer of oxide scale of SN-KO5 powder showed lower α-phase (mass %) than bottom part. It is thought that a lot of liquid phase at top layer attributed α to β transform.[28-45] On the contrary, in case of SN-F2 packing powder, a lot of α-phase (mass %) remained at the top of oxide scale. The reason for this case is not so clear. It might be thought to be due to SN-F2 is β-Si_3N_4-type that never been fully reported in detail on the reverse transform from β to α. Therefore, β to α transformation mechanism in the case of SN-F2 might be abnormal and still in doubt.

4.7.3   Specimens

4.7.3.1 Mixed powder A

α-Contents of specimen and crystal phase in the specimen are shown in Appendices E-5 and E-7. The data of temperature versus α contents are shown in Fig 4.9. It is indicated that only sintering temperature and time affected α to β transformation. The kind of packing powder did not affect α to β transformation.
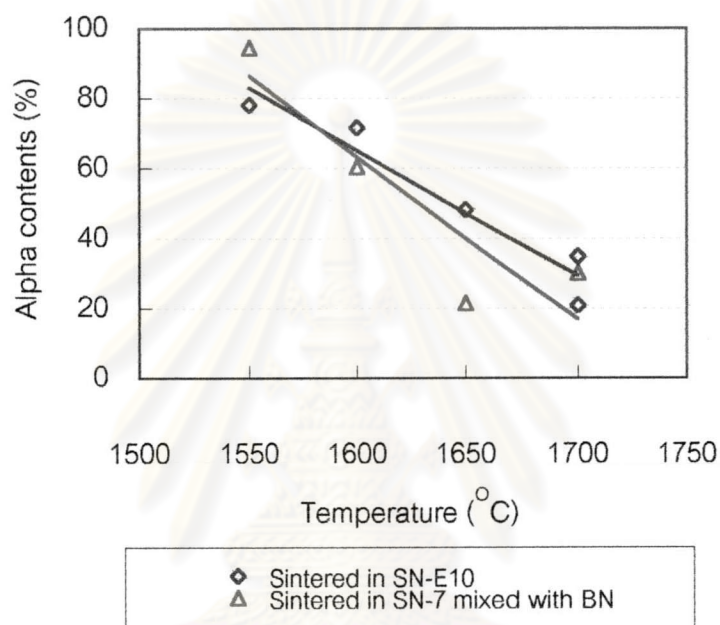

Fig 4.9 Alpha phase content of mixed powder A specimens

4.7.3.2 Mixed powder B

The α -phase (Wt %) contents of each specimen, which sintered in SN-KO5 and SN-F2 packing powders, are shown in Appendix Table E-6. Fig 4.10 shows the temperature effect of α to β transformation rate. The α -phase contents of specimen packed with SN-KO5 were higher than those with SN-F2. At present, the reason has not yet been clarified.
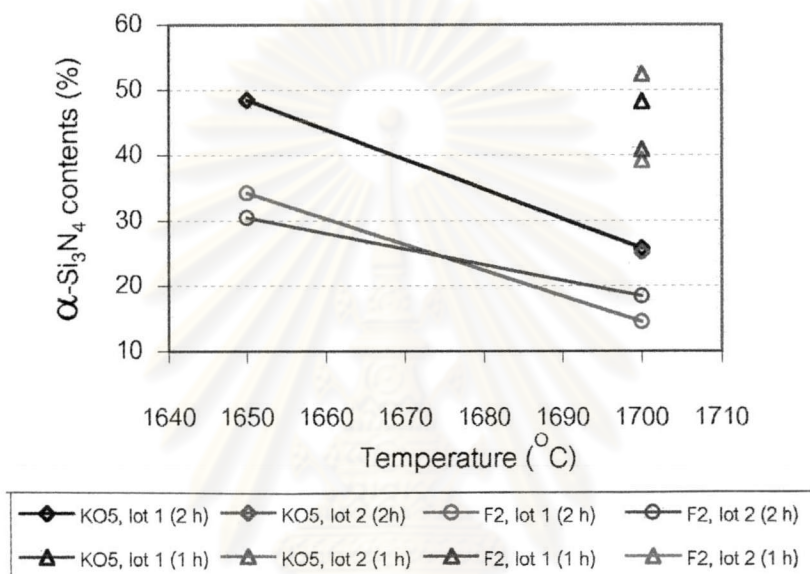

Fig 4.10 Alpha phase content of mixed powder B specimens

Crystal phase in specimen is shown in Appendix Table E-8. Small secondary phases (X_2 and X_3) were observed. In this case, X_2-phase pattern matches with Si_2N_2O pattern, X_3-phase is still unknown because any X-ray pattern of computer does not match.

4.8.　Vickers hardness and fracture toughness

Top views of indent are shown in Fig 4.11. The sizes of the indents and cracks are measured, and the Vickers hardness (Hv) and Fracture toughness (K_{1c}) are calculated by the equation in 3.3.8. The results are shown in Table 4.5.
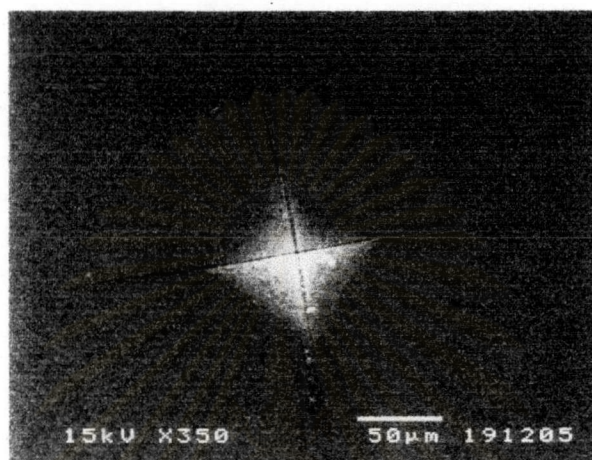
(a)
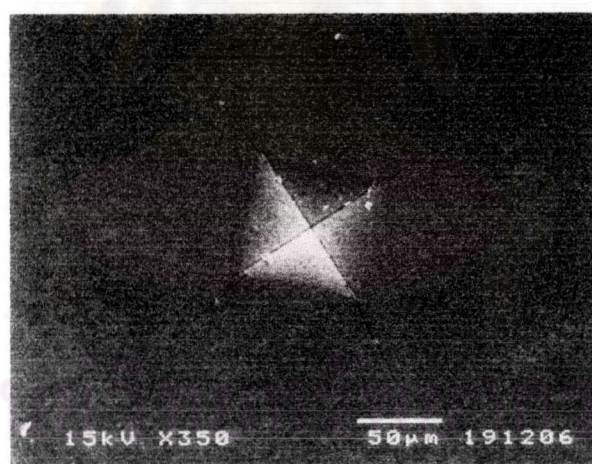
(b)

Fig 4.11 Top view of indents of specimens (a) sintered at 1700 ^{o}C, 1 h soaking, (b) sintered at 1700 ^{o}C, 2 h soaking.

Hv and K_{1C} were measured by two methods. One method is SEM and the other is optical microscope. Details are attached as Appendices Table F-1 and F-2. The value 'of Hv and K_{1C} are a little different by difference of crack measurement. But the differences are not so much.

<u>Table 4.5</u> Hv and K_{1C} of specimens sintered at 1700 ^{o}C for 1 and 2 h.

Specimens (Soaking times)	K_{IC} (MPa.m$^{1/2}$)		Hv (GPa)		α-content (%)	Bulk density (%)
	SEM	Microscope	SEM	Microscope		
1 h	4.7	5.2	17.4	16.6	39	3.16
2 h	5.0	5.1	15.9	15.7	18	3.18

Despite the higher Hv of 1 h specimen, its lower density, resulted from the much amount of α-phase Si_3N_4.

The K_{1C} values in Table 4.5 are calculated by the equation recommended by JIS R 1607.[38] This equation is derived assuming the crack is median cracks. Dr. Niihara[45] reported that the crack will be palmqvist crack as shown in Fig 4.12 when c/a ratio is smaller than 3.5.
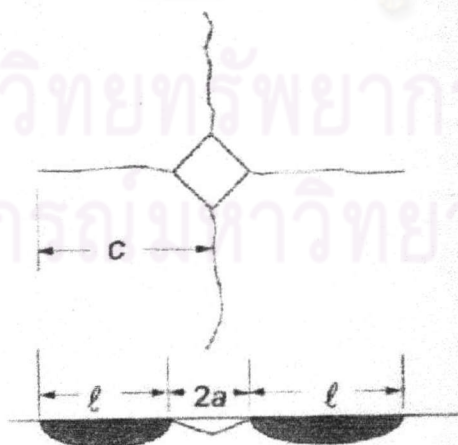

Fig 4.12 The schematic of Plamqvist crack[45]

The c/a values in our experiment are all less than 3.5. The K_{1C} values calculated for median and palmqvist crack are shown in Table 4.6. Statistic examination demonstrates that the values assuming Palmqivst crack have more deviation than that of median crack. Thus, the median crack data is more reliable.

Table 4.6 Comparison of K_{1C} data calculated from the equation assuming of median crack (M) and Plamqvist crack (P)

Condition	OM		SEM	
	M	P	M	P
1 h	5.17 ± 0.03	7.06 ± 0.37	4.66 ± 0.13	6.51 ± 1.31
2 h	5.14 ± 0.05	7.67 ± 0.38	5.00 ± 0.01	5.17 ± 0.37

In Appendix G, properties of TOSHIBA's specimen are shown. Comparing the Hv 16.0 GPa and K_{1C} 5.0 MPa. $m^{(1/2)}$ to the results of our specimens, Hv 16-17 GPa and K_{1C} 4.7-5.0 MPa. $m^{(1/2)}$, the data of our specimens are similar to that of TOSHIBA.

4.9. Flexural strength

Flexural strength was measured for 2 lots, each contained 7 specimens. Details are attached as Appendix F-3. The strength minimum value was 250 MPa and maximum was 506 MPa with an average strength of 427, 414 MPa, respectively.
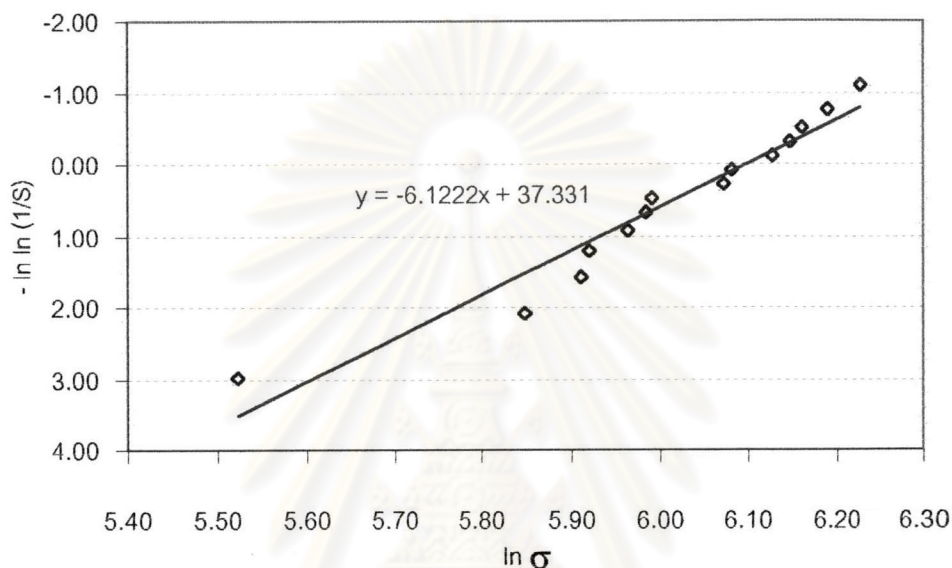

$$y = -6.1222x + 37.331$$

Fig 4.13 Weibull plots of flexural strength at 25 ^{o}C

A Weibull plot of both lots is shown in Fig 4.13. The average strength was 420 MPa, Weibull modulus (m) is 6.1, and a standard deviation is 67 MPa. This m value cause S a surviving stress σ = 144 MPa.

The value of average strength 420 MPa is a little lower than that of commercial one, 600-700 MPa. The causes are thought as follows:

1. Much amount of glass phase

As seen in Table 3.7, the oxygen content in the mixed powder increased from 4.31 mass % to 7.06 mass %. As the result of increased SiO_2 content from 1.69 mass %

to 6.90 mass %. Then the total content of SiO_2, Y_2O_3, and Al_2O_3 increased to 16.9 mass %. It is reported that increasing the glass phase makes the strength lower.[36]

2.   Remaining of α-phase

High aspect ratio morphology is one important factor to make flexural strength high. High aspect ratio is attained after perfect transformation of α-Si_3N_4.[28, 36] The crystal phase of the specimen included about 18 % α-Si_3N_4 as seen in Table 4.5. This remaining of α-Si_3N_4 was due to the limitation of furnace temperature (1700 $^\circ$C).

4.10.   Surface observation by Scanning electron microscope (SEM)

Fig 4.14 and Fig 4.15 show the appearance of the fractured surface morphology. The α-phase percentage for each morphology is 52 (14a), 25 (14b), 39 15(a) and 18 (15b) as shown in Appendixes Table E-6. It has been known that α-phase is equiaxial and β-phase is elongated or needle-like. It was analyzed by XRD that these specimens were composed of α-Si_3N_4, β-Si_3N_4, Si_2N_2O and a small amount of unknown phase (4.7.3)

Fig 4.16(a) and (b) show the morphology of polished surface. There are needle like crystals in Fig 4.16(a). In Fig 4.16(b), large black acicular crystal, small gray needle like crystals and small gray equaiaxial crystals are observed. From these micrographs, it is concluded that big crystal in Fig 4.14 to 4.16 might be Si_2N_2O. Small needle like crystals, which are clearly observed in Fig 4.15(a), (b) and Fig 4.16 (b), will be β-Si_3N_4.

The size of Si_2N_2O is 1-2 μm in diameter and about 10 μm in length. On the other hand, α-Si_3N_4 and β-Si_3N_4 grains are very small. The length of β-Si_3N_4 is about 1 μm. The diameters of α-Si_3N_4 and β-Si_3N_4 are less the 0.5 μm.
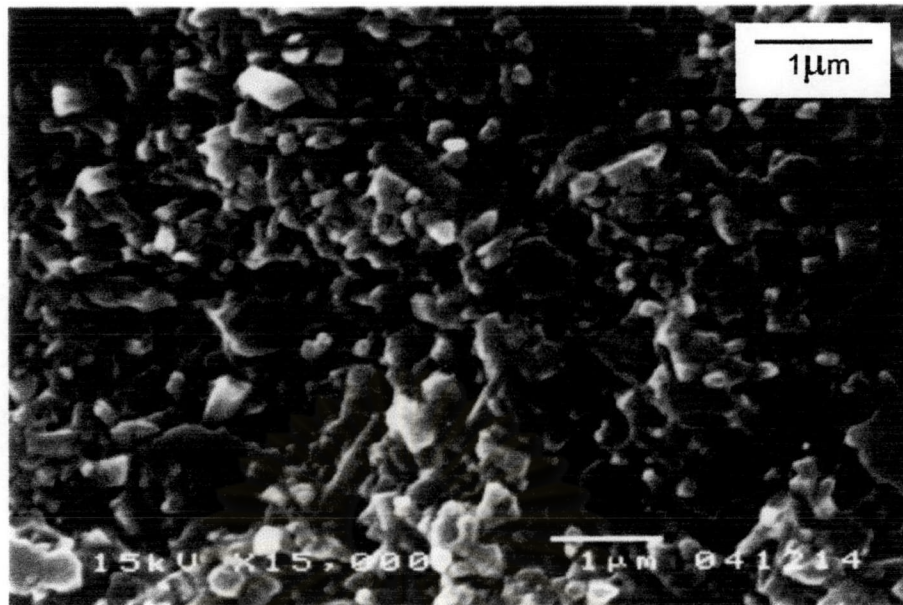
(a)
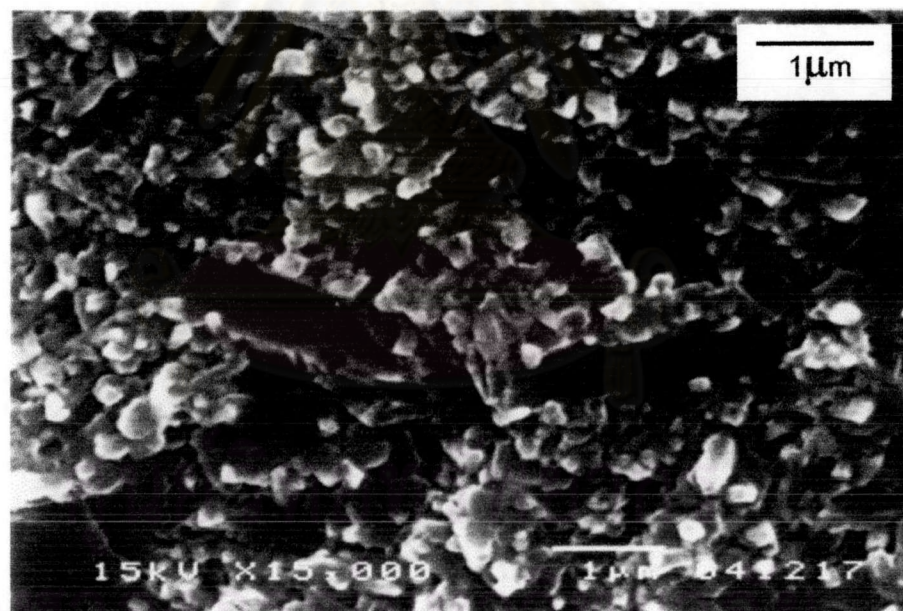
(b)

Fig 4.14 SEM results of mixed powder B (lot 2) sintering at 1700 ^{o}C, 10 ^{o}C/min
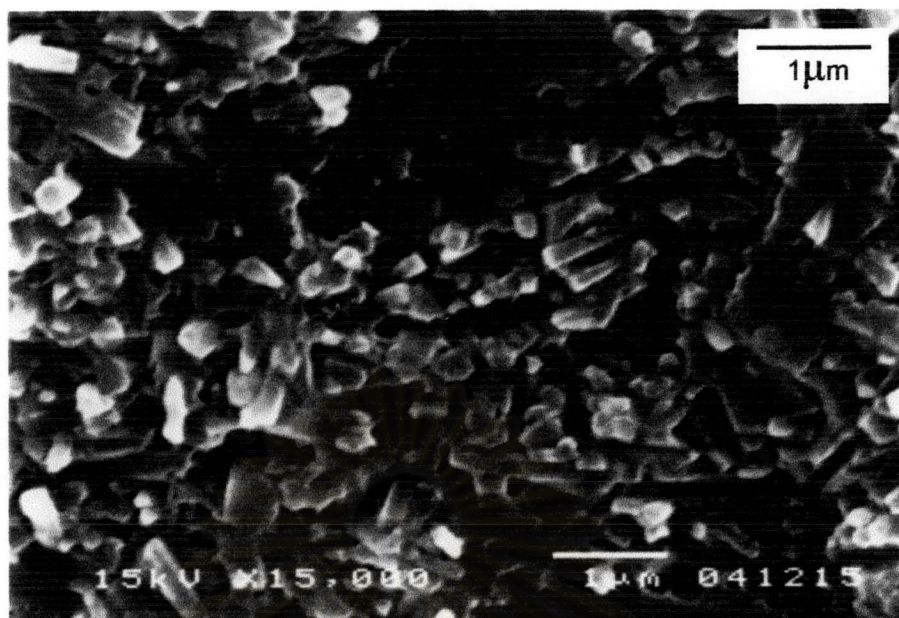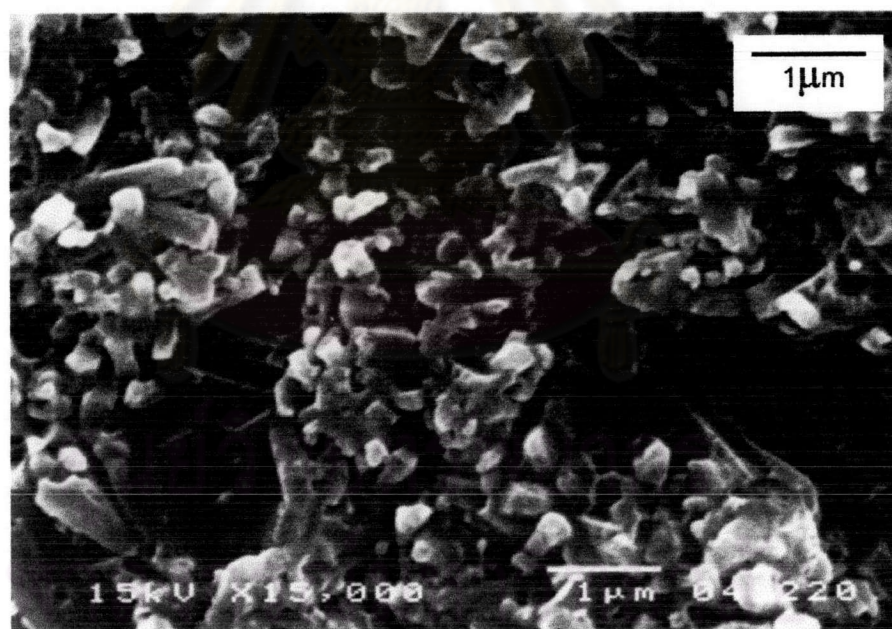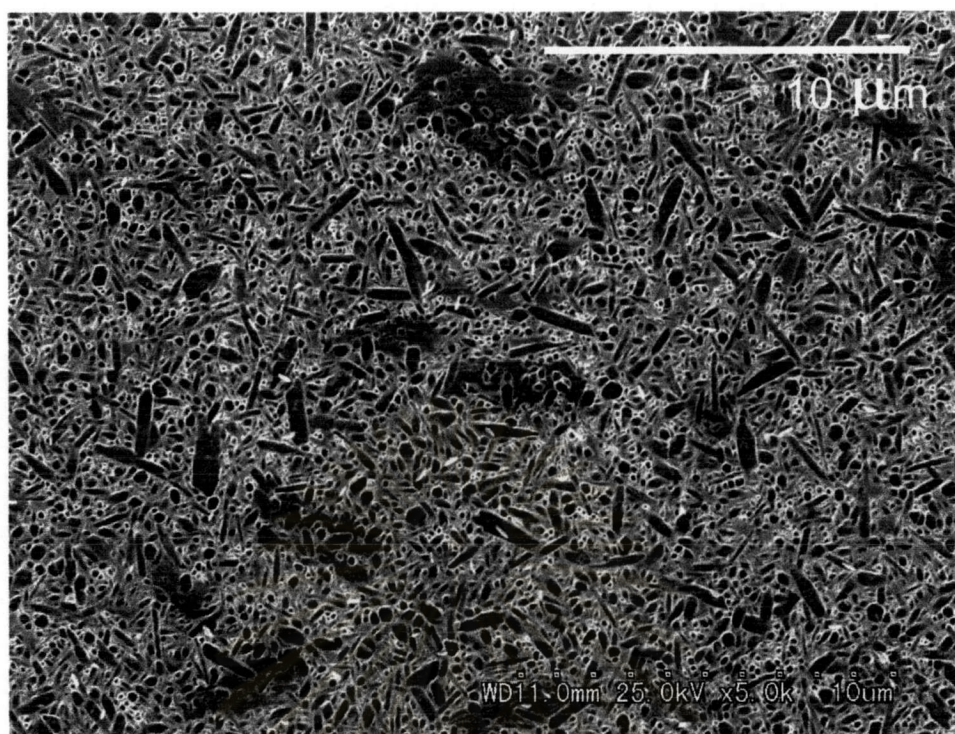with SN-KO5 packing powder a) 1 h soaking b) 2 h soaking
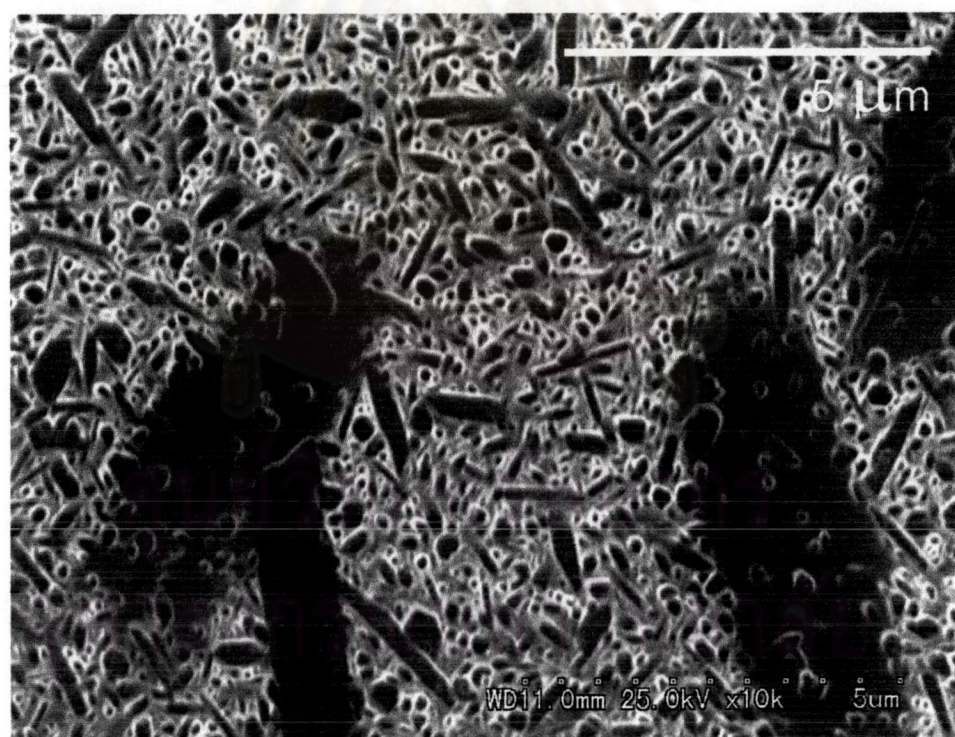
(a)

(b)

<u>Fig 4.15</u> SEM results of mixed powder B (lot 2) sintering at 1700 ^{o}C, 10 ^{o}C/min with SN-F2 packing powder a) 1 h soaking b) 2 h soaking

(a)

(b)

Fig 4.16 SEM micrograph of plasma etched specimen sintered at 1700 ^{o}C, 1h soaking in SN-F2 packing powder.